Figure S1a. Computed structures for $[Zn(Gly\text{-}H)(Gly)]^+$ complexes.

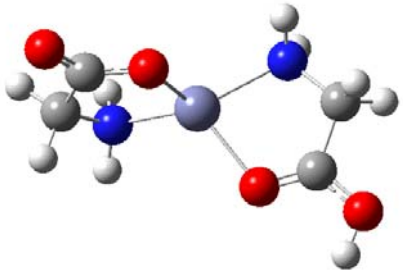

gN1
0/0
0/0

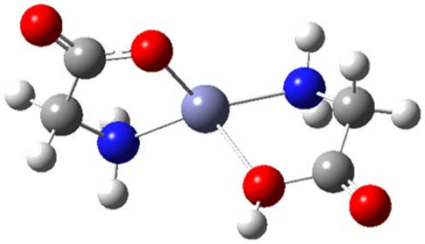

gN2
51.9/52.6
48.1/48.8

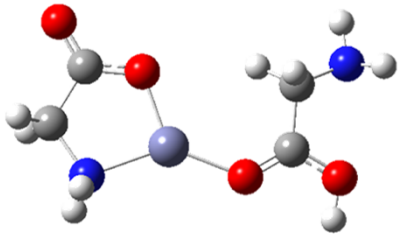

gC
94.1/87.0
101.0/93.9

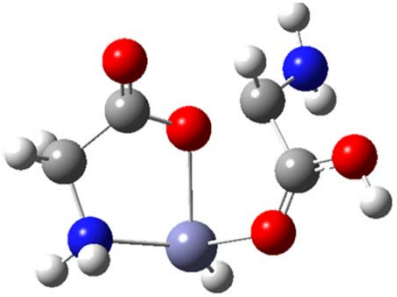

gZ
146.4/152.1
154.2/159.9

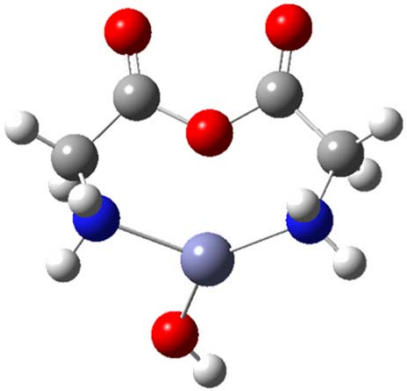

gOH
119.9/120.8
104.4/105.3

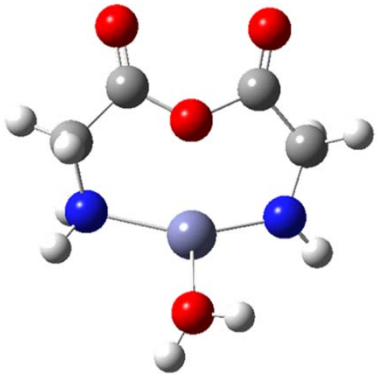

gH2O
176.9/172.3
160.5/155.9

Figure S1b. Computed transition structures for $[Zn(Gly\text{-}H)(Gly)]^+$ complexes.

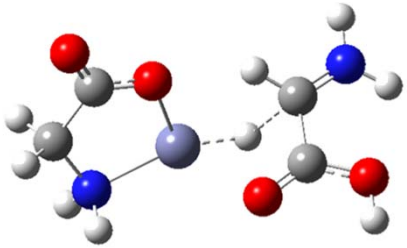

TSg-H1
230.0/230.0
256.3/256.3

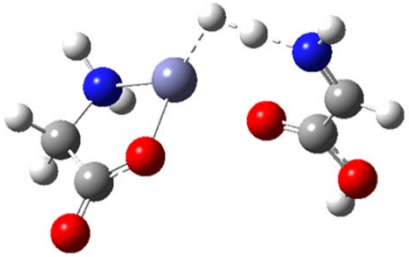

TSg-H2
228.6/226.1
248.1/245.6

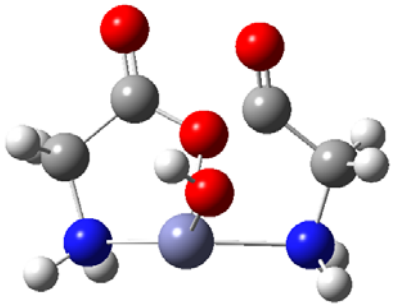

TS-gw1
194.3/205.1
166.2/177.0

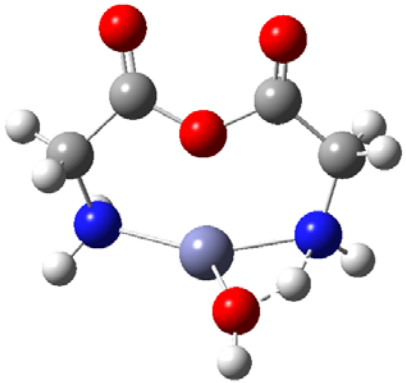

TS-gw2
196.0/202.6
182.1/188.6

Figure S2a. Computed structures for $[Zn(Pro\text{-}H)(Pro)]^+$ complexes.

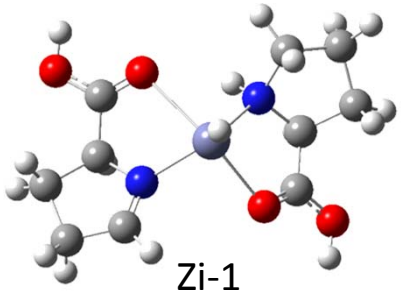

Zi-1
59.1/47.6
85.2/73.7

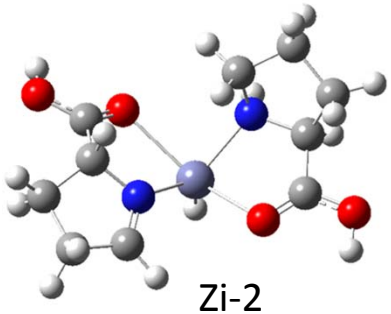

Zi-2
62.5/52.4
85.3/75.2

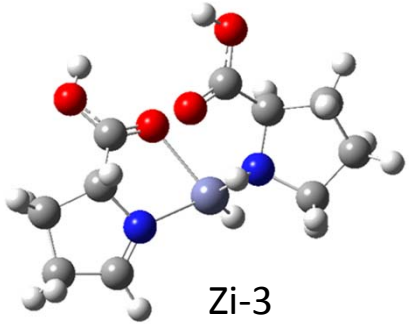

Zi-3
66.9/58.8
88.6/80.5

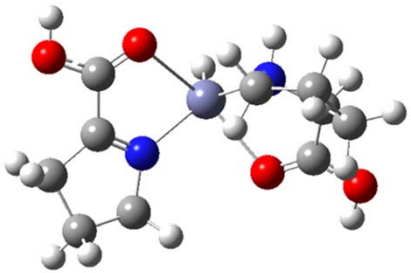

Zii-1
59.3/50.5
83.7/75.0

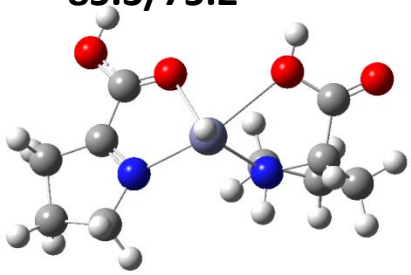

Zii-2
101.5/86.7
126.7/112.0

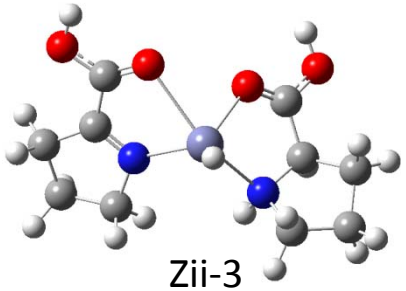

Zii-3
71.8/60.8
100.8/89.8

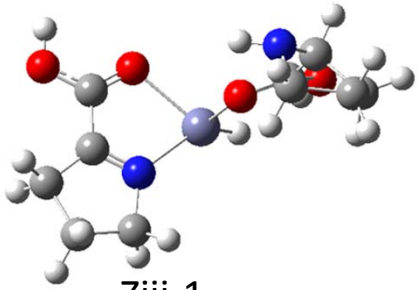

Ziii-1
111.5/94.0
154.0/136.6

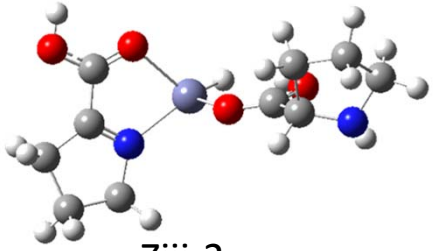

Ziii-2
111.2/96.1
154.3/139.3

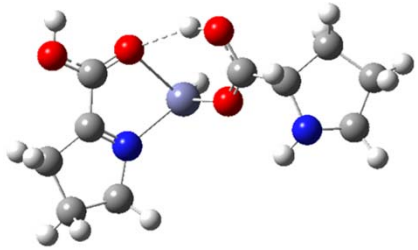

Ziii-3
117.5/103.1
163.7/149.3

Figure S2b. Computed structures for $[Zn(Pro\text{-}H)(Pro)]^+$ complexes.

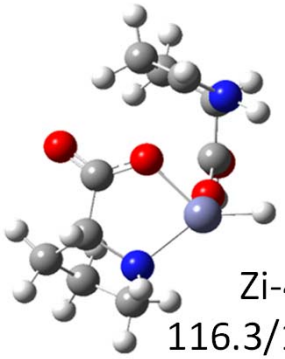

Zi-4
116.3/109.5
145.8/139.0

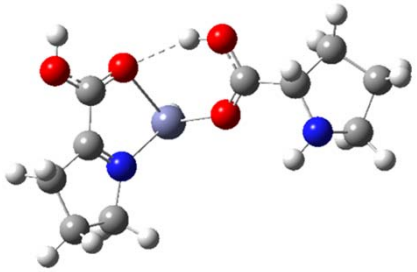

Ziii-4
126.9/110.1
169.1/152.2

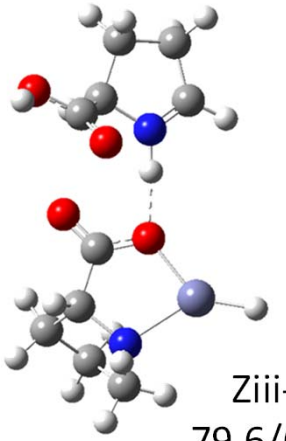

Ziii-5
79.6/64.2
117.3/101.8

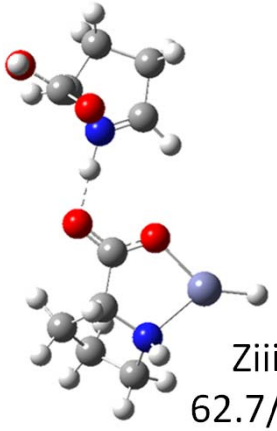

Ziii-6
62.7/47.5
108.1/92.8

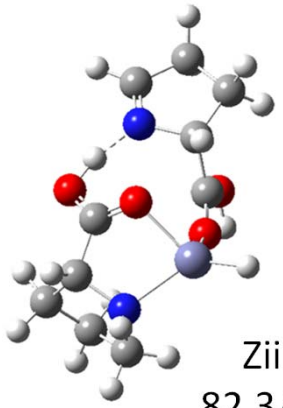

Ziii-7
82.3/77.6
111.5/106.7

Figure S2b. Computed structures for $[Zn(Pro\text{-}H)(Pro)]^+$ complexes.

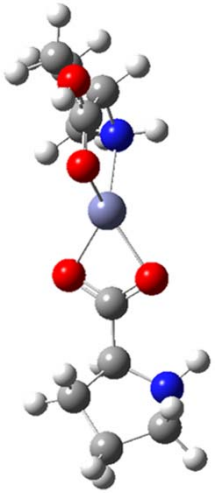

O1
31.4/23.2
50.2/42.0

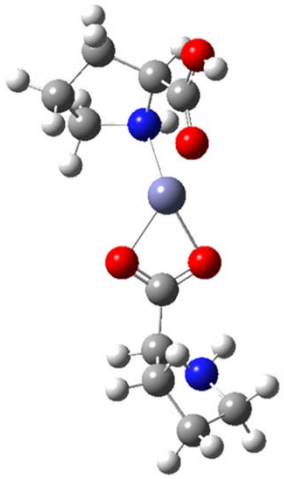

O2
33.0/24.0
50.1/41.3

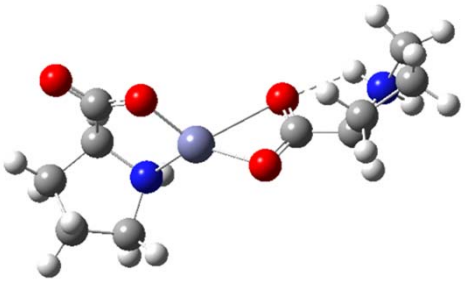

O3
54.6/47.8
69.8/63.0

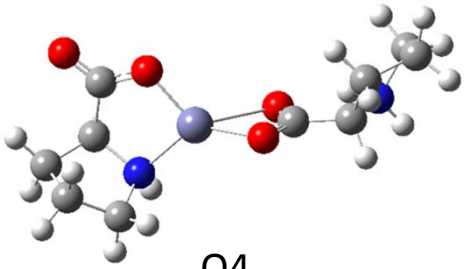

O4
10.6/0.1
27.2/16.7

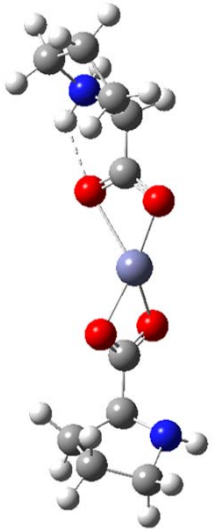

O5
43.9/29.7
70.3/56.0

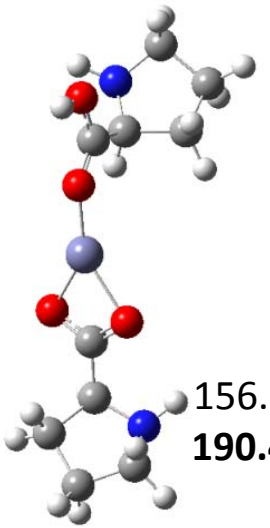

O6
156.2/137.1
190.4/171.2

Figure S2c. Computed structures for $[Zn(Pro\text{-}H)(Pro)]^+$ complexes.

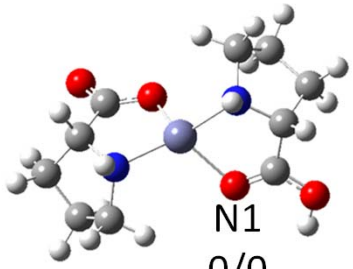

N1
0/0
0/0

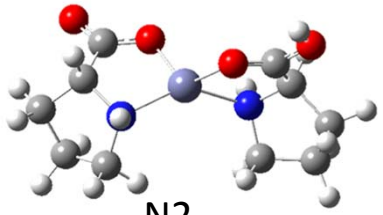

N2
-0.9/2.3
1.6/1.6

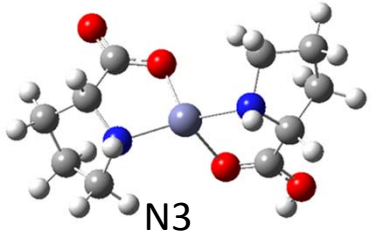

N3
4.8/2.1
10.3/7.5

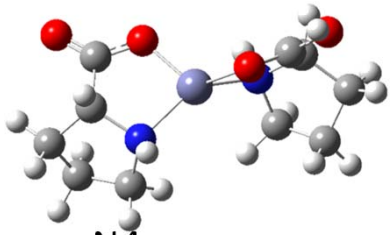

N4
8.5/6.9
12.9/11.3

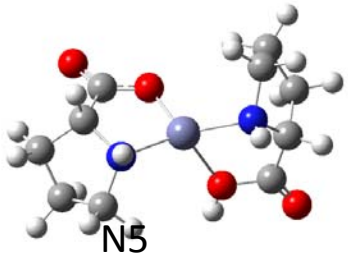

N5
41.8/48.1
49.2/45.4

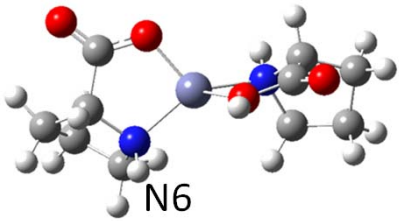

N6
55.4/48.2
55.7/48.5

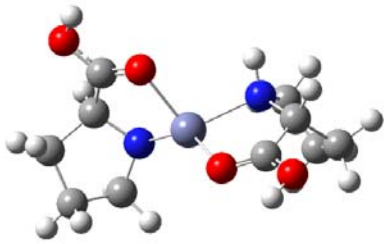

62.9/57.0
68.2/62.3

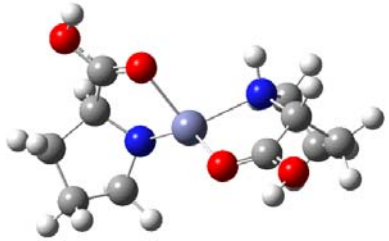

N8
58.8/54.5
64.7/60.3

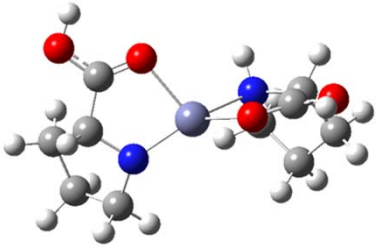

N9
66.8/64.1
78.4/75.8

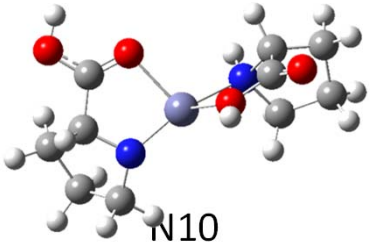

N10
98.9/88.1
102.2/91.4

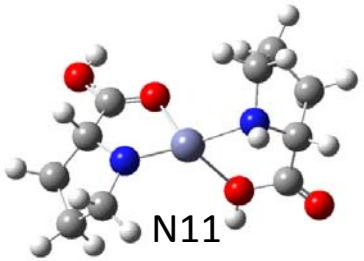

N11
103.6/93.9
46.1/36.4

Figure S2d. Computed structures for $[Zn(Pro\text{-}H)(Pro)]^+$ complexes.

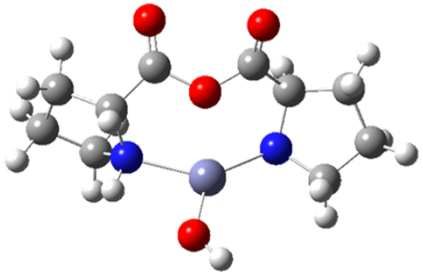

r1
123.5/115.6
117.7/109.9

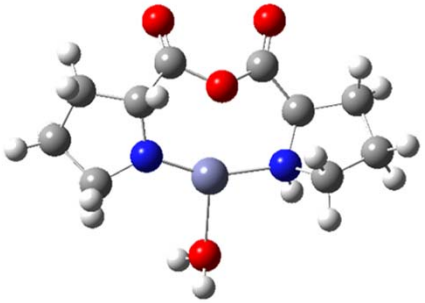

r2
197.0/180.9
188.1/174.2

Figure S2d. Computed transition state structures for $[Zn(Pro\text{-}H)(Pro)]^+$ complexes.

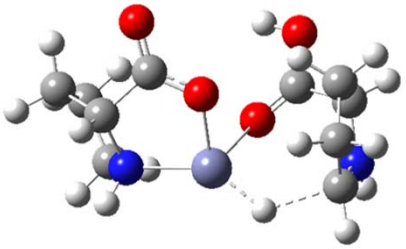

TS-pH1
161.9/0158.4
191.7/188.2

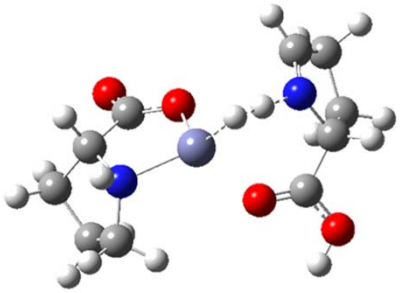

TS-pH2
167.3/161.0
190.4/184.2

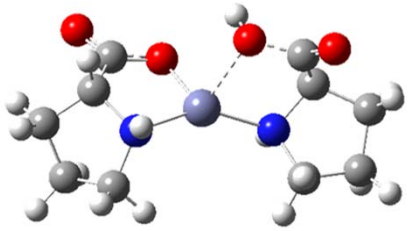

TS-pw1
159.2/167.9
191.0/199.7

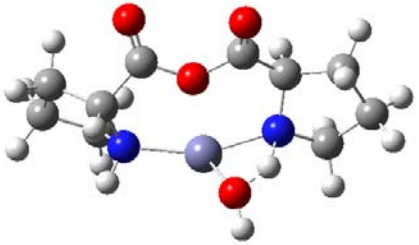

TS-pw2
215.4/214.0
205.6/204.1

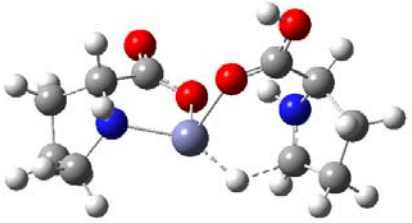

TS-pp
149.3/148.4
181.3/180.4

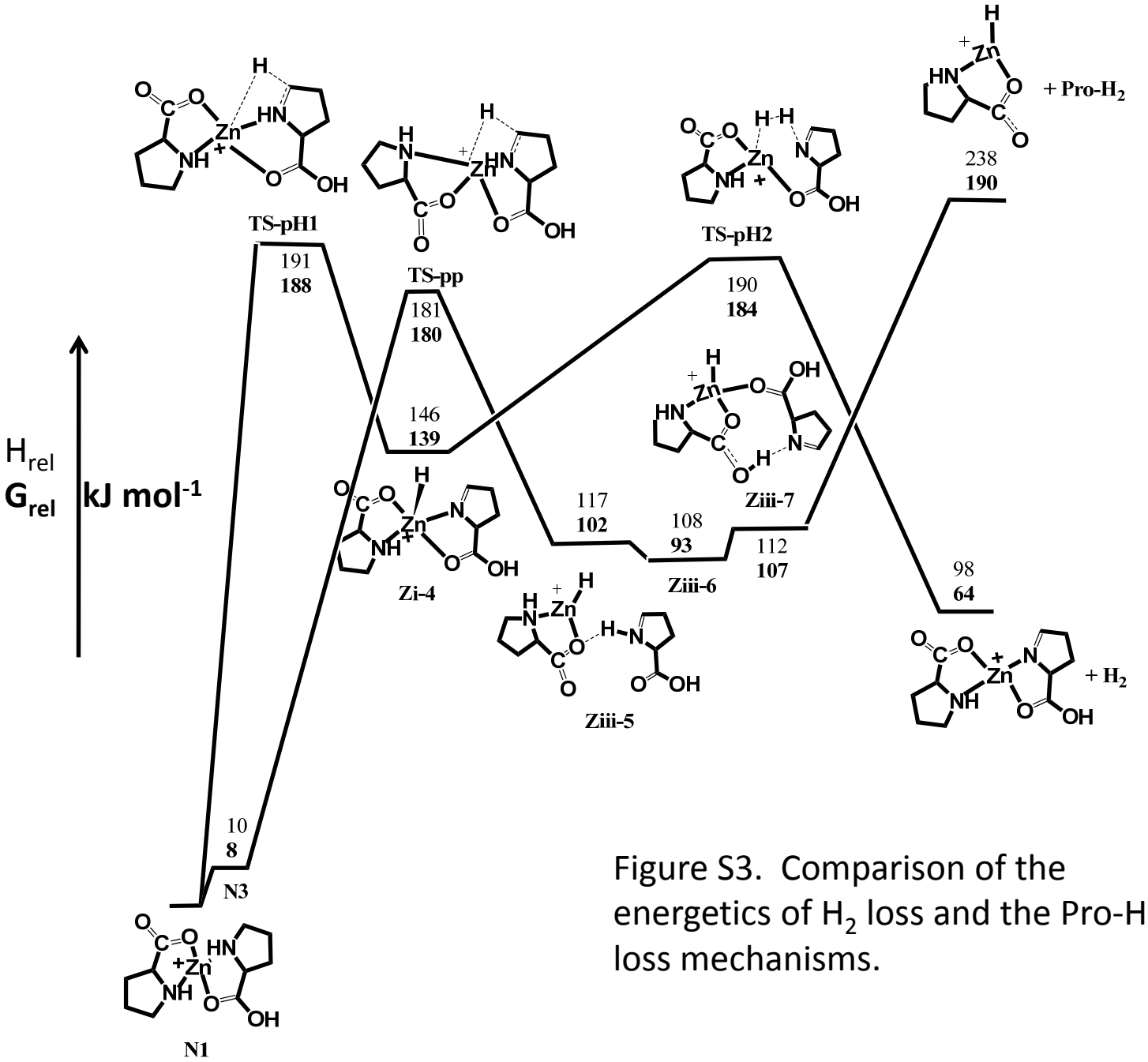

Figure S3. Comparison of the energetics of H_2 loss and the Pro-H_2 loss mechanisms.

Figure S4. Comparison of fragmentation induced by infrared multiphoton activation.

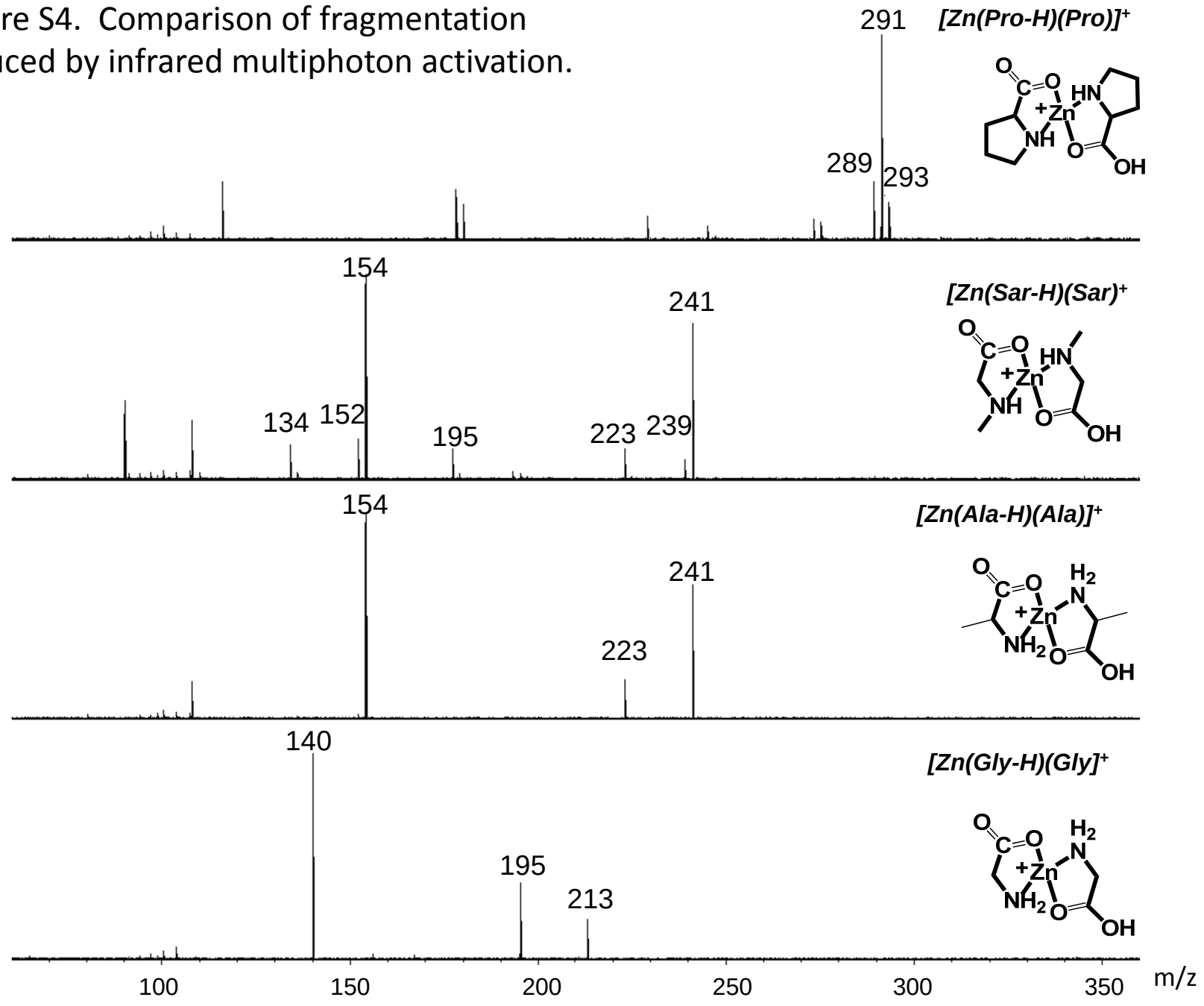

Figure S5

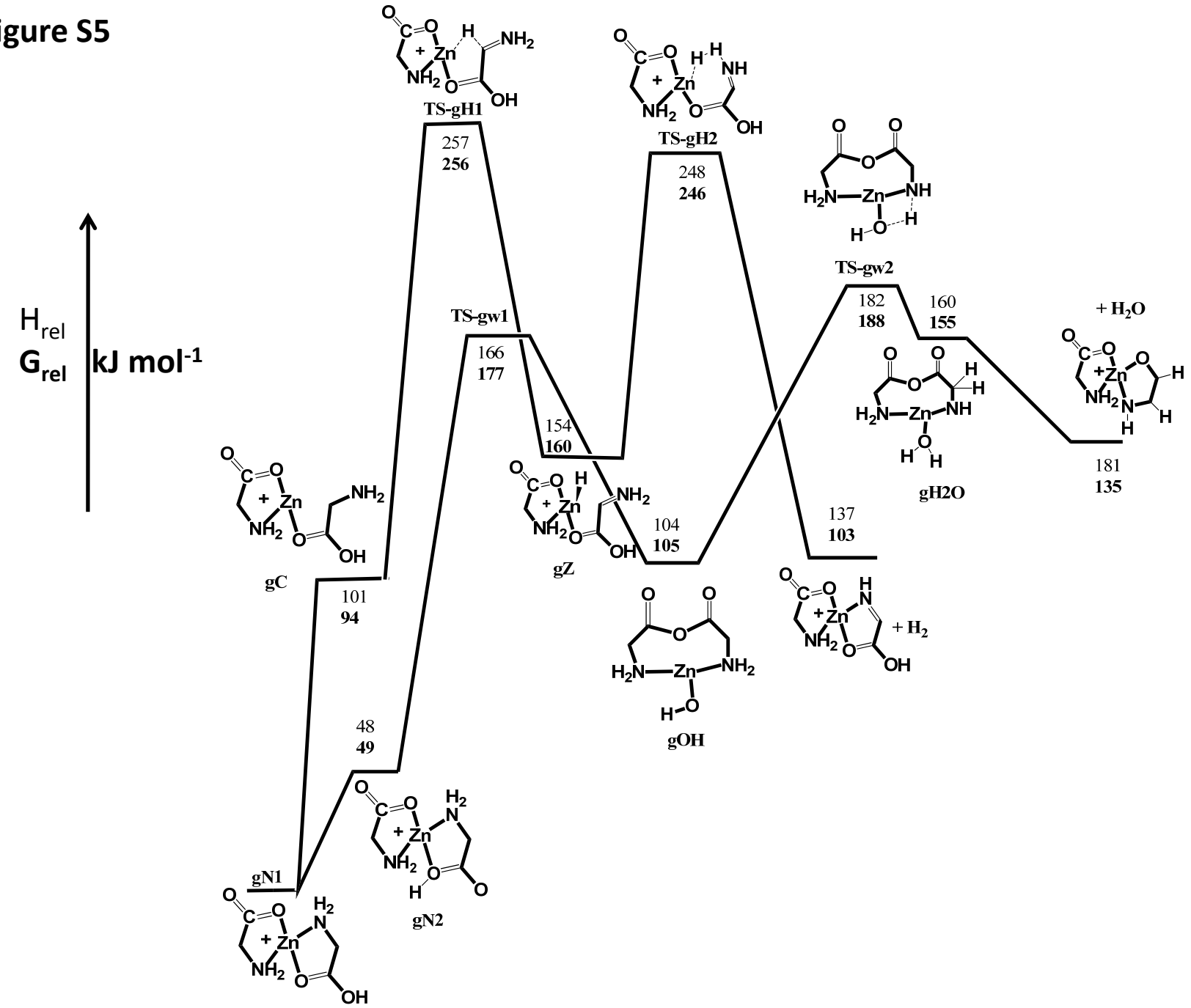

Figure S6. SORI/CID of m/z 180 isolated after CID of m/z 293.

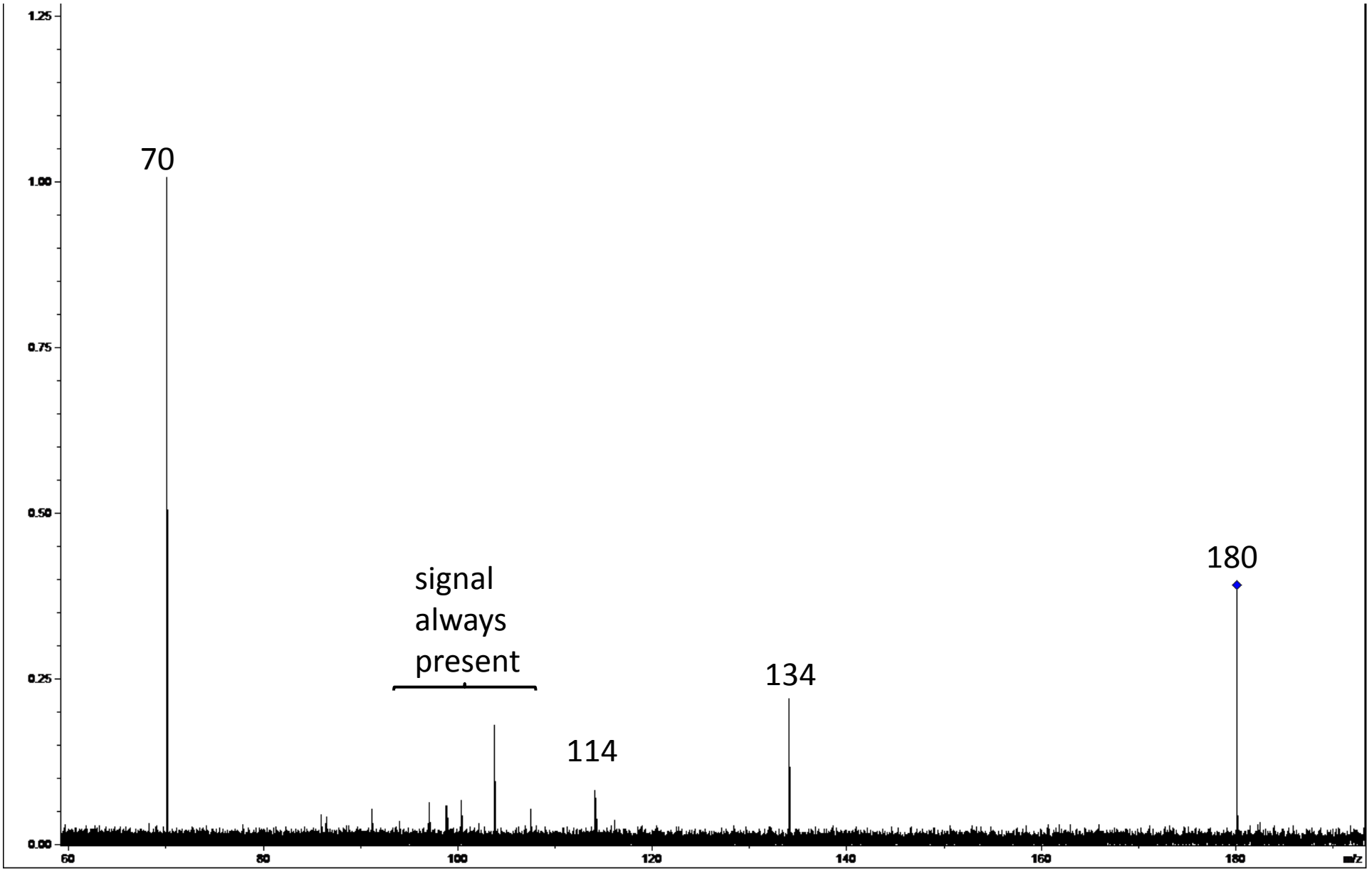

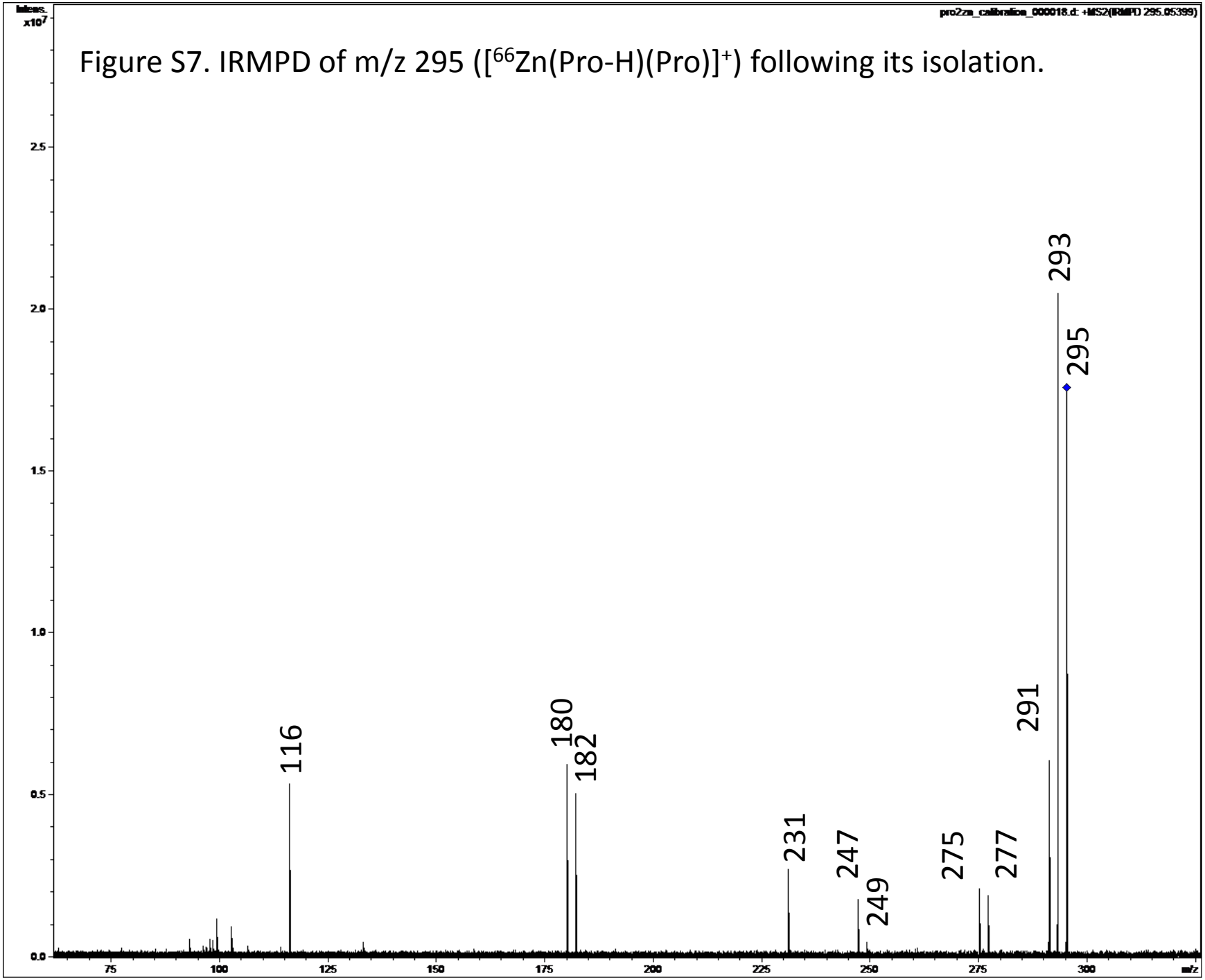

Figure S7. IRMPD of m/z 295 ([^{66}Zn(Pro-H)(Pro)]$^{+}$) following its isolation.

Figure S8. a) SORI MS of m/z 178 formed SORI of ([Zn(Pro-H)(Pro)]$^+$) and b) SORI MS of m/z 181 formed from SORI of ([Zn(2,5,5-d_5-Pro-H)(2,5,5-d_5-Pro)]$^+$). The dissociation of this ion is the topic of JPCB, 2013